A simplified method to evaluate the swelling capacity evolution of a bentonite barrier related to geochemical transformations

G. Montes-H [a,*], B. Fritz [a], A. Clement [a], N. Michau [b]

[a] *UMR 7517 ULP-CNRS, CGS, 1 rue Blessig, F-67084 Strasbourg, France*
[b] *ANDRA, 1/7 rue Jean Monnet, 92298 Châtenay-Malabry Cedex, France*

Abstract

Bentonites have been proposed as buffer material for barriers in geological disposal facilities for radioactive waste. This material is expected to fill up by swelling the void between the canisters containing the waste and the surrounding ground. However, the bentonite barriers may be submitted to changes of humidity, temperature variation, fluid interaction, mass transport, etc. This could modify the physico-chemical performance of the barrier, mainly on the interface with the steel container and with the geological barrier. The engineered barrier development necessitates thus the study of the physico-chemical stability of its mineral component as a function of time under the conditions of the repository in the long-term. The aim of this paper is to apply a simplified method (volume balance in a saturated medium) to evaluate the swelling capacity evolution of a bentonite barrier because of their geochemical transformations by using a thermo-kinetic hydrochemical code (KIRMAT: Kinetic Reactions and Mass Transport "1D").

The system modelled here consists of 1 m thick zone of water-saturated engineered barrier. This non-equilibrated system is placed in contact with a geological fluid on one side, which is then allowed to diffuse into the barrier, while the other side is kept in contact with iron-charged solution (0.001 mol/kg H_2O). The initial reducing conditions ($P_{O_2} \cong 0$; $Eh = -200$ mV) and a constant reaction temperature (100 °C) were considered.

In the current study the decay of swelling capacity was considered directly proportional on the volume of transformed montmorillonite (cation exchange + geochemical transformation), taking into account that it may be partially compensated by the volume of neo-formed swelling-clays.

The results showed that the swelling capacity of the engineered barrier is not drastically affected after about 3000 years of reaction and transport because the volume of neo-formed swelling clays is almost directly proportional on the volume of transformed montmorillonite. In fact, a graphical method predicted that the decay of swelling capacity of the engineered barrier lies between 11% and 14% when the montmorillonite is completely transformed (cation exchange + minimal geochemical transformation) in the system.

---

* Corresponding author. Fax: +33 3 90 24 04 02.
E-mail addresses: montes@illite.u-strasbg.fr, german_montes@hotmail.com (G. Montes-H).

1. Introduction

One of the radioactive waste disposal designs proposes to confine the waste in deep impervious clay geological layers. Vitrified waste is laid in canisters in the middle of a gallery dug in the clay formations. In order to protect canisters from water intrusion and to eventually delay the release of radioelements, waste-forms will be isolated from the surrounding geological media by two barriers: (a) the steel canister and (b) an engineered backfill barrier system. This backfill barrier will be essentially composed of compacted clay blocks because of the hydro-dynamic and surface properties of clay materials. In addition, due to swelling characteristics, the buffer material is expected to fill up the spaces between the canisters containing the waste and the surrounding ground, and to build up a better impermeable zone around high-level radioactive waste. This role is called as "self-sealing" (Komine, 2004; Komine and Ogata, 2003).

The MX80 bentonite contains about 85% in volume of Na/Ca-montmorillonite and 15% of accessory minerals (Sauzeat et al., 2001). The dominant presence of montmorillonite in this clay mineral should give an excellent performance as engineered barrier in the radioactive waste repository because of its swelling property (see Fig. 1). However, the Na/Ca-montmorillonite may be transformed to other clay minerals as a function of time (on the long-term). Several previous simulations have shown that the Na/Ca-montmorillonite-to-Ca-montmorillonite conversion was the more significant chemical transformation, i.e. the chemical transformation from a medium-swelling clay to a low-swelling clay. Globally, this process represents a significant cation exchange in the barrier. The neo-formation of chlorites (non-swelling clays) was also observed as a potential chemical transformation particularly near from iron container (Kluska et al., 2002; Montes-H et al., 2004) (see Fig. 2).

Taking into account the previous results, the aim of this paper is to apply a simplified method (volume balance in a saturated medium) to evaluate the swelling capacity decay of bentonite barrier because of their geochemical transformations by using the thermo-kinetic hydrochemical code (KIRMAT: Kinetic Reactions and Mass Transport "1D", Gérard et al., 1998).

The system modelled here consists of 1 m thick zone of water-saturated engineered barrier. This non-equilibrated system is placed in contact with a geological fluid on one side, which is then allowed to diffuse into the barrier, while the other side is kept in contact with iron-charged water (0.001 mol/kg H_2O) (Fig. 3). Initial reducing conditions ($P_{O_2} \cong 0$; $Eh = -200$ mV) and a constant reaction temperature (100 °C) were considered. Finally, in the current study the decay of swelling capacity was considered directly proportional on the volume of transformed montmorillonite (cation exchange + geochemical transformation), taking into account that it may be
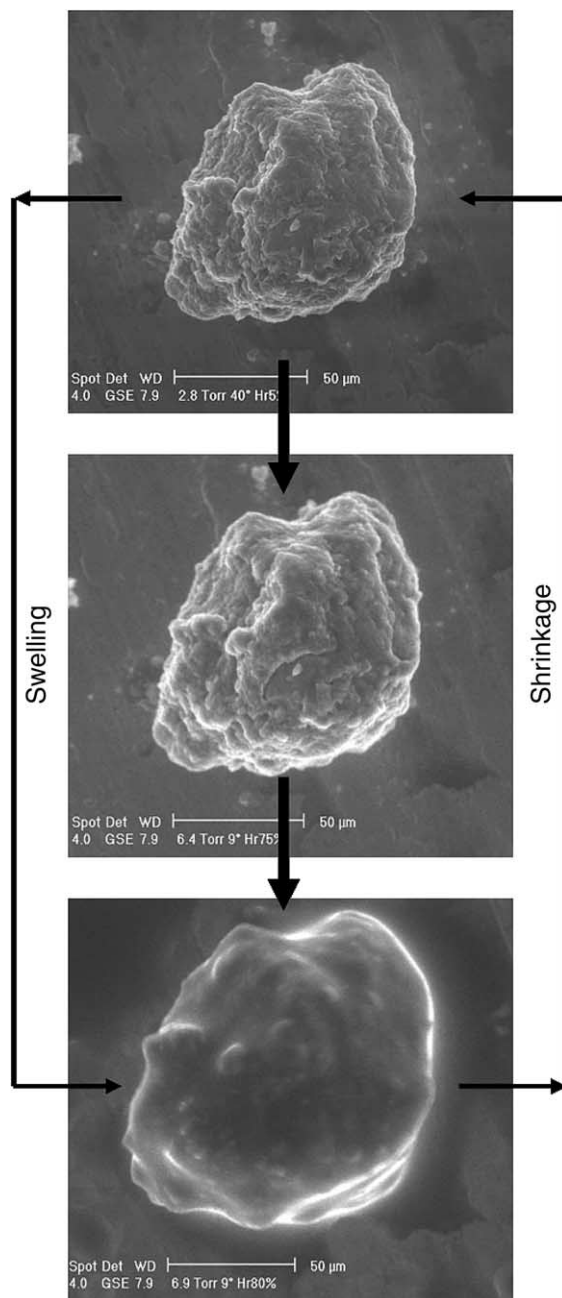

Fig. 1. Swelling property of MX80 bentonite (Montes-H, 2002).

partially compensated by the volume of neo-formed swelling-clays in the system (see Eq. (2)).

2. Model description

The Eulerian thermo-kinetic hydrochemical code KIRMAT (Gérard et al., 1998) has been developed from
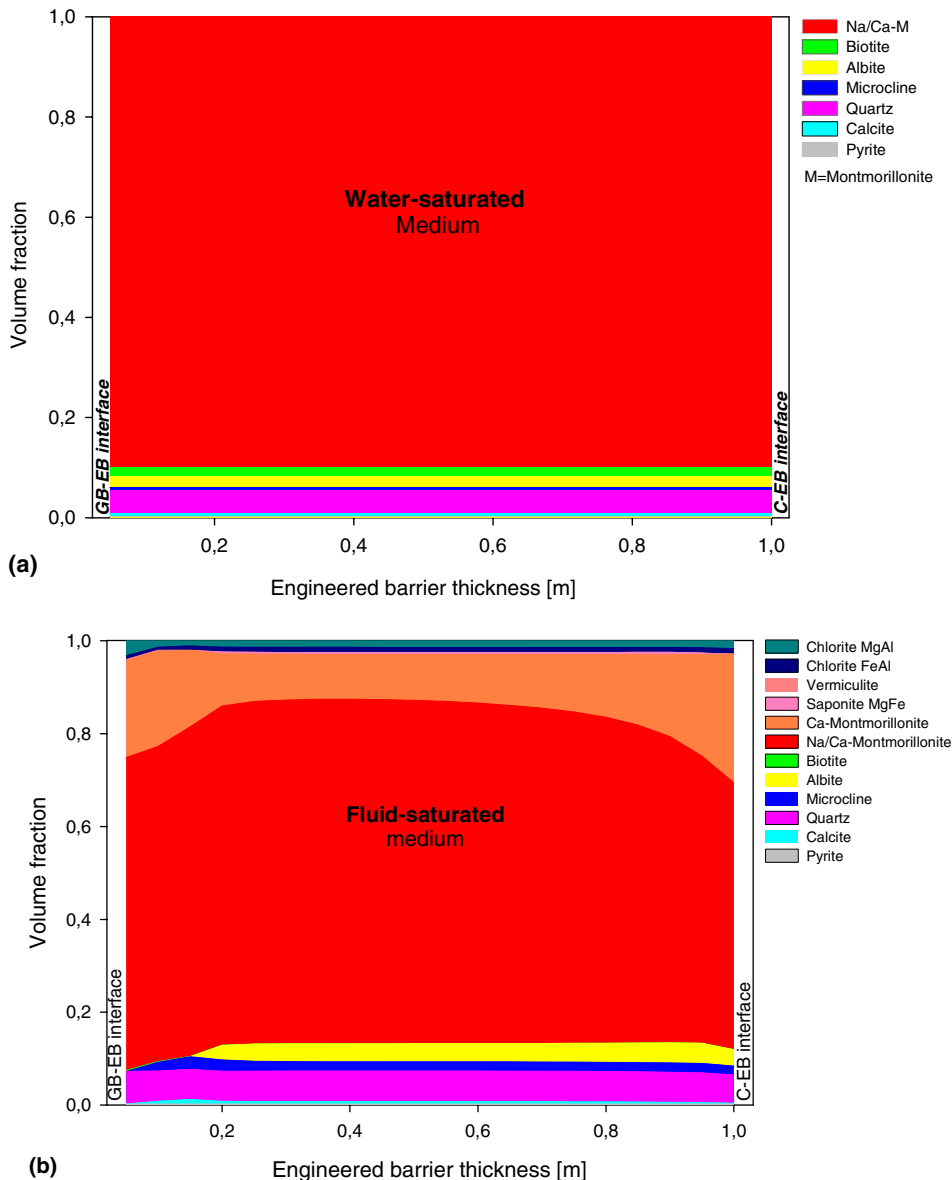
Fig. 2. (a) Mineral composition of the engineered barrier at water-saturated conditions (initial state). (b) Mineral composition of fluid-saturated engineered barrier after 1000 years of reaction and transport.

the reaction path model KINDIS (Madé et al., 1994), by keeping all its geochemical formulation and its numerical method to solve chemical equations.

The thermo-kinetic geochemical code KINDIS had been developed from the purely thermodynamic code DISSOL (Fritz, 1975; Fritz and Tardy, 1976; Fritz, 1981), which in turn originated from PATH1 (Helgeson et al., 1970). Theoretical kinetic rate laws for mineral dissolution and precipitation based on the transition state theory (TST) have been implemented in DISSOL. These geochemical codes have been intensively numeri-cally tested and used in published studies on hydrothermal, diagenetic and weathering processes (e.g., Noack et al., 1993; Bertrand et al., 1994).

In KINDIS, the irreversible kinetic driving force is explicitly calculated and the sequence of partial equilibrium state is calculated from second-order Taylor series expansion (Madé et al., 1994).

In KIRMAT, solute transport is added to kinetic dissolution and/or precipitation reactions. A chemically controlled time step (noted Δt_c) allows to preserve accuracy of the calculations. Its value is chosen inversely
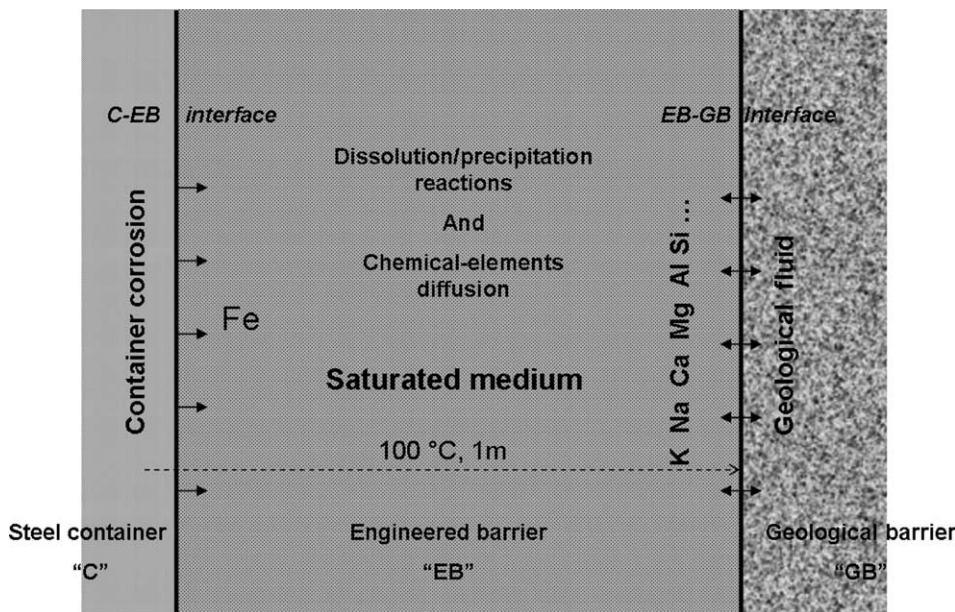
Fig. 3. Schematic representation of fluid-rock interaction and solute diffusion in an engineered barrier for radioactive waste confinement.

proportional to the largest of the first derivative variations among all the solute concentrations, and is controlled by setting the θ parameter (inversely proportional to Δt_c). The set of the partial differential equations is integrated along one direction with the classical finite difference approximation method. An explicit scheme and a one-step algorithm are used to solve simultaneously the chemical (from KINDIS) and the conservative transport mass balance equations. A classical mixing cell scheme, the explicit-backward discretization, is computed for a numerical validation study with the property of interest. It involves less numerical dispersion than the other mixing cell scheme (Bajracharya and Barry, 1993).

The coupling of chemical reactions with mass transport is now currently reported in the literature. Unfortunately, it is still difficult to take into account all physico-chemicals phenomena in a system (Poinssot et al., 1998; Collin et al., 2002; Gens et al., 2002; Keijzer et al., 1999; Malusis and Shackelford, 2002; Ulm et al., 2002; Le Gallo et al., 1998; Savage et al., 2002; Hökmark et al., 1997; Källvenius and Ekberg, 2003).

3. Methodology

3.1. General considerations

All simulations presented here were performed using version 1.6 of the thermo-kinetic hydrochemical code KIRMAT. The main interest was to simulate the long-term geochemical transformations of the engineered barrier (hydrolysis reactions) taking into account the chemical-elements diffusion (Fe, K, Ca, Na, Mg, etc.) in order to evaluate their decay of swelling capacity. The following aspects were considered to simplify the modelling system.

(i) Geochemical transformations in *fluid-saturated medium*. A recent study showed that a bentonite barrier will be fully water-saturated within about 3 or 4 years after deposition (Hökmark, 2004). Then, it was supposed that the interface contact "engineered barrier-geological medium" operates as a permeable membrane only to the water during the hydration phase of engineered barrier. In this case, the chemicals species contained in the geological fluid will be only adsorbed (or retarded) in the first centimeters of the engineered barrier. These comments allow to assume that initially the engineered barrier is saturated with a fluid lowly concentrated. In this study, the engineered barrier is initially saturated with pure water.

(ii) Solute *diffusion*. In the water-saturated engineered barrier of bentonite the interstitial fluid is almost static because the very low permeability in the medium. In these conditions the convection transport can be negligible. Then, the significant transport phenomena through the engineered barrier is

uniquely the chemical-elements diffusion; mainly the iron-diffusion toward the geological medium and the K, Ca, Na, Si, etc. diffusion toward the metallic container.

(iii) *Reducing conditions*. Here, it was admitted that after the closing of the repository system, the hydrolysis reactions of mineral constituents of the engineered barrier take place in reducing conditions ($P_{O_2} \cong 0$; $Eh = -200$ mV) because the oxygen is supposed to be rapidly consumed.

(iv) *Container corrosion*. In the KIRMAT code, at the moment it is difficult to take into account directly the container corrosion. For that, a significant concentration (100 times superior to the estimated concentration in the natural site "Callovo-Oxfordian") of total iron (0.001 mol/kg H_2O) was considered in the boundaries of container. This means that one side of engineered barrier is perturbed by a constant source of iron during the simulation. Unfortunately, this assumption could produce an acidification phenomenon in the system.

(v) *Initial state* of the engineered barrier. The engineered barrier was considered initially in disequilibrium with the interaction solution (pure water) therefore this system is initially very reactive.

3.2. Conceptual system

The system modelled here consists of 1 m thick zone of water-saturated engineered barrier of bentonite. This non-equilibrated system is placed in contact with a geological fluid on one side, which is then allowed to diffuse into the barrier, while the other side is kept in contact with iron-charged solution. This configuration represents the contact of the engineered barrier with a geological medium and with a container in a geological disposal facility for radioactive waste (Fig. 3).

A grid spacing of 5 cm was used for all the calculations reported (i.e. the thickness of engineered barrier was divided into 20 grids).

3.3. A simplified method to evaluate the swelling capacity decay

In general, in the water-saturated bentonite barrier the specific (grain) densities of non-swelling minerals keep constant. In contrast, the specific (grain) densities of swelling minerals decrease because of their expansive property. Therefore, the specific (grain) density of a water-saturated swelling-clay can be calculated by the following expression:

$$\rho_{sw\_clay}^{wet} = \rho_{sw\_clay}^{dry}\left(\frac{1+W}{1+\frac{w}{1-w}+S_w}\right), \tag{1}$$

with $\rho_{sw\_clay}^{dry}$: specific (grain) density of a dried swelling clay. This value was estimated by using helium adsorption method (picnometry) for a bulk sample of MX80 bentonite (Sauzeat et al., 2001). In the current study, this value was considered as characteristic for any swelling clay;

W: maximal amount of adsorbed water. These values were estimated by using the sorption kinetic of water vapour (relative humidity = 95%) (Montes-H and Geraud, 2004). In this study, it was assumed that the Ca-montmorillonite and the saponites have the same capacity to adsorb the water vapour;

w: total physical porosity. This value was estimated by using the Hg-porosimetry for a bulk sample of MX80 bentonite (Sauzeat et al., 2001). In this study, this value was considered as characteristic for any swelling clay;

S_w: the maximum swelling potential was estimated by using a new technique of environmental scanning electron microscopy (ESEM) coupled with a digital image analysis (DIA) program (Montes-H et al., 2003). In this study, it was assumed that the Ca-montmorillonite and the saponites have the same capacity to swell.

The values used in the current study are summarized in Table 1. It is necessary to remark that any swelling clay was supposed to contribute to fill up the total physical porosity (see Fig. 4). In this case, the interstitial fluid is almost static because the very low permeability in the medium. For that, only the molecular diffusion could be possible in the engineered barrier.

Table 1
Several physical properties of swelling clays

Swelling clay	$\rho_{sw\_clay}^{dry}$ [g/cm^3]	W [g/g$_{dry\ clay}$]	w [cm^3/cm^3]	S_w [cm^3/cm^3]	$\rho_{sw\_clay}^{wet}$ [g/cm^3]	Molar mass [g/mol]	Molar volume [cm^3/mol]
Na/Ca-S	2.65	0.3	0.3	0.14	2.19	372.61	170
Na-S	2.65	0.37	0.3	0.3	2.10	373.14	178
Ca-S	2.65	0.25	0.3	0.09	2.18	371.96	171
Saponites	2.65	0.25	0.3	0.09	2.18	440.45[a]	202

$\rho_{sw\_clay}^{dry}$: specific (grain) density of a dried swelling clay.
W: maximal amount of adsorbed water.
w: Total physical porosity. S_w: the maximum swelling potential.
$\rho_{sw\_clay}^{wet}$: specific (grain) density of a hydrated swelling clay.
S: montmorillonite (and/or smectite).
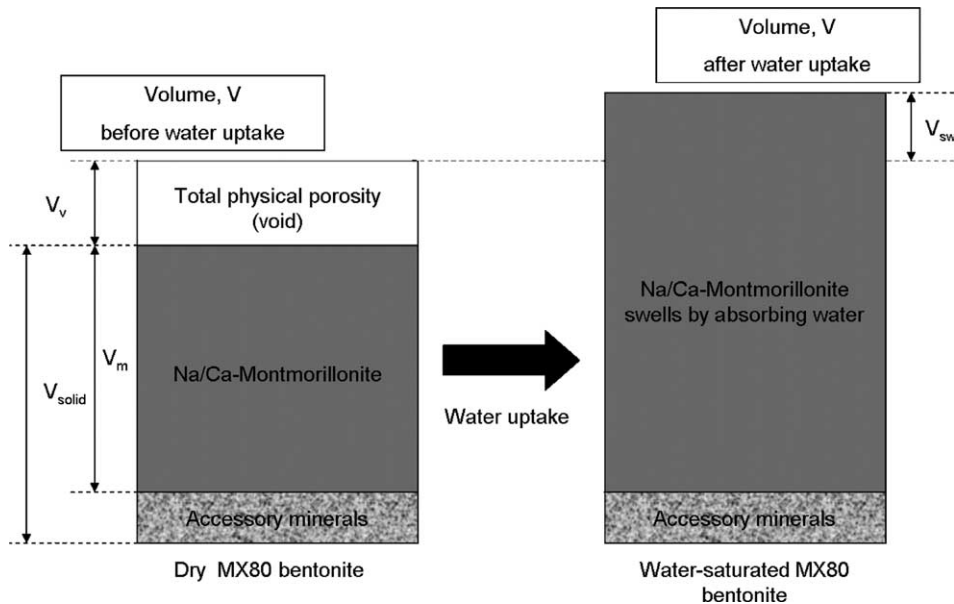[a] Mean value between five different saponites.

Fig. 4. Definition of MX80 bentonite barrier at water-saturated conditions (after Komine and Ogata, 2003).

In the other hand, it was assumed that accessory minerals contained in the bulk bentonite do not affect on the maximum swelling S_w and on the maximal amount of adsorbed water W.

The specific (grain) density calculation of water-saturated swelling-clays allows to estimate their molar volume. This parameter is therefore used in the KIRMAT code to calculate the mineral volume in the system. This simple correction allow to estimate the evolution of the swelling capacity by a volume balance calculation considering that the decay of swelling capacity is directly proportional on the volume of transformed montmorillonite (cation exchange + geochemical transformations), taking into account that it may be partially compensated by the volume of neo-formed swelling-clays. The calculation is then based in the following equation:

$$D = \left(1 - \frac{V_{d\_swell\text{-}clay}}{V_{i\_system}}\right) + \frac{\sum V_{p\_swell\text{-}clay}}{V_{i\_system}}, \quad (2)$$

where $V_{d\_swell\text{-}clay}$ is the volume of the swelling-clay dissolved, $V_{p\_swell\text{-}clay}$ the volume of the swelling-clay precipitated, V_{i_system} the initial volume of the swelling-clay in the system.

4. Input data

4.1. Primary minerals

The MX80 bentonite has been widely studied (Sauzeat et al., 2001; Guillaume, 2002; Montes-H, 2002; Montes-H et al., 2003, 2004; Tournassat et al., 2003; Neaman

et al., 2003 and others). This commercial clay mineral contains about 85% of Na/Ca montmorillonite and 15% of accessory minerals (see Table 2). In our study the minerals of the MX80 bentonite are considered as primary minerals or as reactants for possible chemical transformations. In the KIRMAT simulations, the chemical transformation of primary minerals was treated with a kinetic option. In contrast, their re-precipitation was considered with a thermodynamic equilibrium option (local equilibrium assumption).

4.2. Secondary minerals

The secondary minerals or neo-formed mineral phases were chosen following the conclusions of the laboratory experiments conducted at 80 and 300 °C in the presence of metallic iron (Guillaume, 2002). In Table 3 are summarized the secondary minerals considered in this study. In this case, the mineral neo-formation was treated with a thermodynamic option (i.e. at equilibrium condition).

4.3. Initial composition of the fluid

The engineered barrier is considered as a saturated medium, initially saturated with pure water. In contrast, the geological fluid was a representative geological fluid of the French Callovo-Oxfordian formation (see Table 4).

4.4. Temperature of reaction

In the KIRMAT code it is not possible to take into account the temperature gradient as a function of time

Table 2

Mineral composition of MX80 bentonite (Sauzeat et al., 2001); and thermodynamic equilibrium constants used in KIRMAT simulations

Mineral	Volume fraction (dry bentonite)	Volume fraction water-saturated bentonite	Chemical formula	Log(K_m) (100 °C)
Pyrite	0.00313	0.002023	FeS_2	−67.89[b]
Calcite	0.00966	0.006245	$CaCO_3$	−9.39[b]
Quartz	0.07032	0.045465	SiO_2	−3.095[b]
Microcline	0.01066	0.006892	$KAlSi_3O_8$	−18.104[b]
Albite	0.03490	0.022564	$NaAlSi_3O_8$	−16.037[b]
Biotite	0.02783	0.017993	$K(Fe_3)[Si_3AlO_{10}](OH)_2$	5.910[b]
Na/Ca-montmorillonite	0.84350	0.898814	$[Si_{3.98}Al_{0.02}O_{10}](OH)_2$ $(Al_{1.55}Mg_{0.28}Fe^{III}_{0.09}Fe^{II}_{0.08})(Na_{0.18}Ca_{0.10})$	−28.455 [a]
Total	1.00000	1.000000		

[a] The sum of polyhedral contributions (Chermak and Rimstidt, 1989, 1990).
[b] Data base of KIRMAT code.

Table 3

Secondary minerals and the thermodynamic equilibrium constants used in KIRMAT simulations

Mineral	Chemical formula	Log(K_m) (100 °C)
Vermiculite MgFe2	$[(Si_{3.67}Al_{0.33}O_{10})(OH)_2](Al_{0.33}Fe^{II}_{1.15}Mg_{1.52})$	−5.14[a]
Saponite Fe(II)	$[(Si_{3.67}Al_{0.33}O_{10})(OH)_2](Fe^{II}_3)Na_{0.33}$	−2.05[a]
Saponite MgFe(II)	$[(Si_{3.5}Al_{0.5}O_{10})(OH)_2](Al_{0.25}Fe^{II}_{1.25}Mg_{1.5})Ca_{0.05}Na_{0.15}$	−2.11[a]
Montmorillonite Na	$[(Si_{3.96}Al_{0.04}O_{10})(OH)_2](Al_{1.52}Fe^{III}_{0.18}Mg_{0.27})Na_{0.4}$	−28.84[a]
Montmorillonite Ca	$[(Si_{3.96}Al_{0.04}O_{10})(OH)_2](Al_{1.52}Fe^{III}_{0.18}Mg_{0.27})Ca_{0.2}$	−29.23[a]
Phillipsite Na	$[Si_{10}Al_6O_{32}]Na_5Ca_{0.5}12H_2O$	−72.05[a]
Laumonite	$[SiAl_2O_8]Ca4H_2O$	−26.38[b]
Chabazite Na	$[Si_8Al_4O_{24}]Na_{3.5}Ca_{0.25}13H_2O$	−51.26[a]
Chlorite FeAl	$[Si_2Al_2O_{10}(OH)_2](Fe^{II}Al_2)(Fe^{II}_3)(OH)_6$	−55.57[a]
Chlorite MgAl	$[Si_2Al_2O_{10}(OH)_2](MgAl_2)(Mg_3)(OH)_6$	−31.23[a]
Illite	$[(Si_{3.5}Al_{0.5}O_{10})(OH)_2](Al_{1.8}Mg_{0.25})K_{0.6}$	−35.23[b]
Goethite	$FeO(OH)$	8.82[b]
Siderite	$FeCO_3$	−11.95[b]
Magnetite	Fe_3O_4	22.65[b]
Anhydrite	$CaSO_4$	−5.36[b]
Gypsum	$CaSO_4.2H_2O$	−5.010[b]
Thenardite	Na_2SO_4	−0.640[b]
Jarosite	$KFe^{III}_3(SO_4)_2(OH)_6$	20.84[b]

[a] The sum of polyhedral contributions (Chermak and Rimstidt, 1989, 1990).
[b] Data base of KINDISP model.

Table 4

Chemical composition, pH and Eh of a representative geological fluid from Callovo-Oxfordian formation (Jacquot, 2002)

Chemical parameters	Value	Observation
Eh [mV]	−185	SO_4/pyrite equilibrium
pH	7.30	Electroneutrality condition
Na [mol/kg H_2O]	4.17×10^{-2}	Na–Ca exchange
K [mol/kg H_2O]	5.40×10^{-3}	K-Ca exchange
Ca [mol/kg H_2O]	9.74×10^{-3}	Equilibrium with calcite
Mg [mol/kg H_2O]	7.68×10^{-3}	Na–Mg exchange
SiO_{2aq} [mol/kg H_2O]	9.44×10^{-5}	Equilibrium with quartz
Cl [mol/kg H_2O]	7.19×10^{-2}	Calculated by lixivation
SO_4 [mol/kg H_2O]	4.40×10^{-3}	$pCO_2 = 3.09 \times 10^{-3}$ condition
Al [mol/kg H_2O]	9.26×10^{-9}	Equilibrium with illite
Fe [mol/kg H_2O]	6.44×10^{-5}	Equilibrium with daphnite
C_T (inorganic) [mol/kg H_2O]	1.44×10^{-3}	Equilibrium with dolomite
pCO_2 [atm]	3.09×10^{-3}	–

due to the disintegration reactions of radioactive waste. However, it is possible to take into account any temperature comprised between 0 and 300 °C. The confinement barrier is subjected to temperature variations (over 70 °C and sometimes over 100 °C) (Collin et al., 2002). In this study, a constant temperature of 100 °C was assumed as Andra's unpublished data suggested that the temperature should be homogeneous shortly after the closure of the repository.

4.5. Initial pH and P_{CO_2}

The P_{CO_2} was initially fixed at 3.16×10^{-4} bar. Knowing that the alkaline reserve is null for the pure water, the initial pH was calculated at 5.89 considering a temperature of 100 °C.

4.6. Water-rock ratio

The total physical porosity of MX80 bentonite was estimated at 30% for a physical density of 1.8 g/cm^3 (Sauzeat et al., 2001). Assuming that the engineered barrier is initially saturated with pure water and knowing that the KIRMAT code is based on one kilogram of water (i.e. approximately 1000 cm^3 "V_{water}"); it is possible to estimate the rock volume of interaction (approximately 2333 cm^3). This value, the mineral volume fraction of the dry bentonite and swelling potential of Na/Ca-montmorillonite allow to calculate the initial volume of each primary mineral in the system.

4.7. Thermodynamic equilibrium constants

The KIRMAT code is based on the hydrolysis reactions where the major aqueous species are mainly H_4SiO_4, $Al(OH)_4^-$, CO_3^{--}, SO_4^{--}, Na^+, K^+, Ca^{++}, Mg^{++}, Fe^{++}, Fe^{+++}, H^+, H_2O. The thermodynamic equilibrium constants of hydrolysis reactions used in

KIRMAT simulations at 100 °C are presented in Tables 2 and 3.

4.8. Kinetic data

The simplified equation used to simulate the dissolution rate of a mineral m in the KIRMAT code may be written as

$$v_{dm}^s = k_{dm}^{pH} S_m^{eff} a_{H^+}^n \left(1 - \frac{Q_m}{K_m} \right), \tag{3}$$

where k_{dm}^{pH} is the constant of the apparent dissolution rate intrinsic to mineral m at a given pH (mol/m^2/year); S_m^{eff} is the effective or reactive surface area (as a function of the number of actives sites) at the mineral/aqueous solution interface (m^2/kg H$_2$O); $a_{H^+}^n$ is the activity of the H$^+$ ions in the aqueous solution, where n is a real exponent with a generally positive value in acid solutions, zero in neutral solutions and negative in basic solutions; and $(1 - Q_m/K_m)$ is the saturation index of mineral 'm' in the aqueous solution, where Q_m is the ionic activity product and K_m is the thermodynamic equilibrium constant known for the given temperature and pressure conditions.

The intrinsic constant of the mineral dissolution (k_{dm}^{pH}) is a function of the temperature which can be described by the Arrhenius law:

$$k_{dm}^{pH} = A_m \exp \left(\frac{-E_{am}}{RT} \right), \tag{4}$$

being A_m, the frequency factor and E_{am}, the activation energy of mineral dissolution reaction (J mol^{-1}).

The k_{dm}^{pH} data used in the current study were taken from compilation made by Jacquot (2000) and Kluska (2001). These values are summarized in Table 5.

On the other hand, the effective or reactive surface area (S_m^{eff}) could be defined as a percentage of the total mineral surface area, generally between 50% and

Table 5
The kinetic data used in the KIRMAT simulations

Mineral	S_m^{eff} [m^2/kg H$_2$O][a]	k_{dm}^{pH} [mol/m^2 year]			pH limit	
		k^{Ha}	k^{H_2Oa}	k^{OHa}	A-to-N	N-to-B
Pyrite	2.19	1.88×10^{-18}	1.88×10^{-18}	1.88×10^{-18}	–	–
Calcite	6.76	7.93×10^6	8.69×10^2	8.69×10^2	4.4	8.3
Quartz	49.22	4.5×10^{-3}	1.7×10^{-3}	3.18×10^{-6}	2	5.5
Microcline	7.46	1.40	7.89×10^{-3}	5.97×10^{-6}	4.5	7.8
Albite	24.42	1.40	7.89×10^{-3}	5.97×10^{-6}	4.5	7.8
Biotite	19.48	1.34×10^{-3}	1.89×10^{-5}	5.45×10^{-7}	5	7
Montmorillonite	590.4	1.34×10^{-3}	1.89×10^{-5}	5.45×10^{-7}	5	7

k^H: constant of the dissolution rate in an acid medium.
k^{H_2O}: constant of the dissolution rate in a neutral medium, independent of the pH.
k^{OH}: constant of the dissolution rate in a basic medium.
S_m^{eff}: reactive surface area. A: acid; N: neutral; B: basic.
[a] Kinetic data (after the compilations Jacquot, 2000 and Kluska, 2001).

90% (White and Peterson, 1990). Recently, the atomic force microscopic experiments showed that only 8–14% of the total mineral surface area participate as reactive surface area (S_m^{eff}) on the dissolution of several silicates (Nagy et al., 1999; Tournassat et al., 2003). In reality it is still difficult to estimate with a good precision, the reactive surface area of silicates and phyllosilicates. The granular studies show that a bulk sample of MX80 bentonite is composed by 86.1% of particles in a size range below 2 μm, 8.8% in the 2–50 μm range and 5.1% of sizes over 50 μm (Neaman et al., 2003). In this study, it was supposed that the MX80 bentonite is composed by particles of size 2 μm. This consideration allows to calculate the total mineral surface area (S_m^T) for each primary mineral. Finally it was also assumed that only 10% of the total mineral surface area participates as reactive surface area ($S_m^{eff} = 0.1 S_m^T$).

The kinetic data (k_{dm}^{pH}, S_m^{eff}) used in the KIRMAT simulations, are therefore presented in Table 5.

4.9. Diffusion coefficient

The transport of solutes into the clay barrier was considered to be a pure diffusion process in a saturated medium. The initial effective-coefficient of diffusion tested in the simulations was 10^{-11} m^2/s. This value was selected based on published data for compacted MX80 (Lehikoinen et al., 1996). The KIRMAT code uses the same value for all chemical species and considers a constant molecular diffusion.

5. Results and discussion

Previous studies carried out by our institute have shown that the chemical transformations occurring in a bentonite barrier for radioactive waste confinement depend directly on the reaction temperature, the rate of iron corrosion, the composition of interaction fluid, the nature and/or amount of accessory minerals, the diffusion coefficients of solutes, the reactive surface area of minerals, etc. (Jacquot, 2000; Kluska, 2001; Kluska et al., 2002; Montes-H et al., 2004). In fact, the Na/Ca-montmorillonite-to-Ca-montmorillonite conversion was identified as the main chemical phenomena in the bentonite barrier, i.e. the chemical transformation from a moderate-swelling clay to a low-swelling clay (see Figs. 2 and 5). A minimal neo-formation of illite, saponites, chlorites and sodium-montmorillonite was also observed. The Na/Ca-montmorillonite-to-Ca-montmorillonite conversion represents a simple cation exchange in the barrier identified indirectly by hydrolysis reactions.

The main interest of this study was then to evaluate the evolution of swelling capacity of the bentonite barrier due to the chemical transformations as a function of time by using the Eq. (2). For this, two scenarios were considered:

(1) A progressive chemical transformation of Na/Ca-montmorillonite with prediction of the *non-swelling minerals neo-formation*. In this case, the decay of swelling capacity of the bentonite barrier is directly
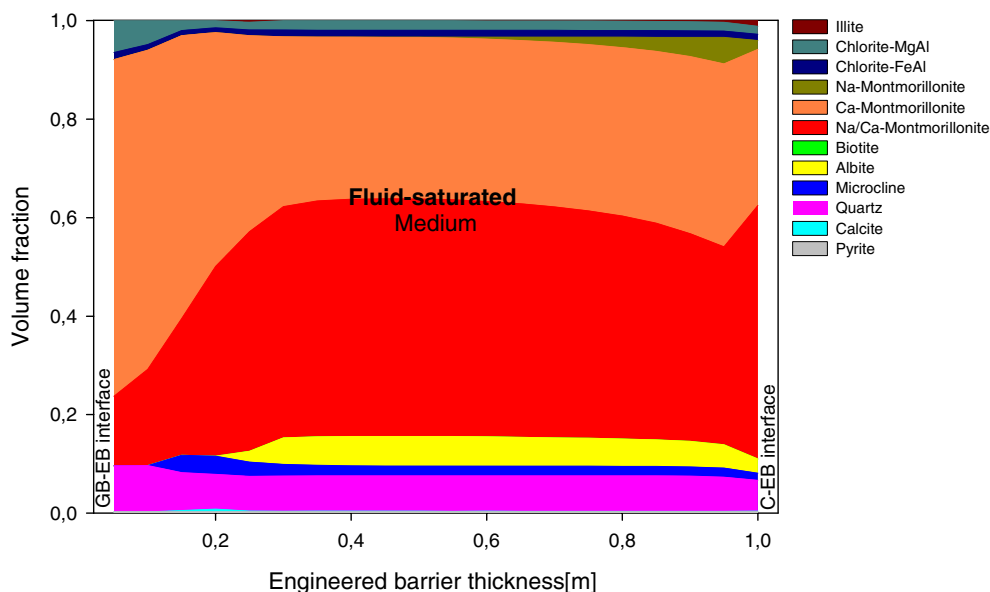

Fig. 5. Mineral composition of fluid-saturated engineered barrier after 3320 years of reaction and transport.
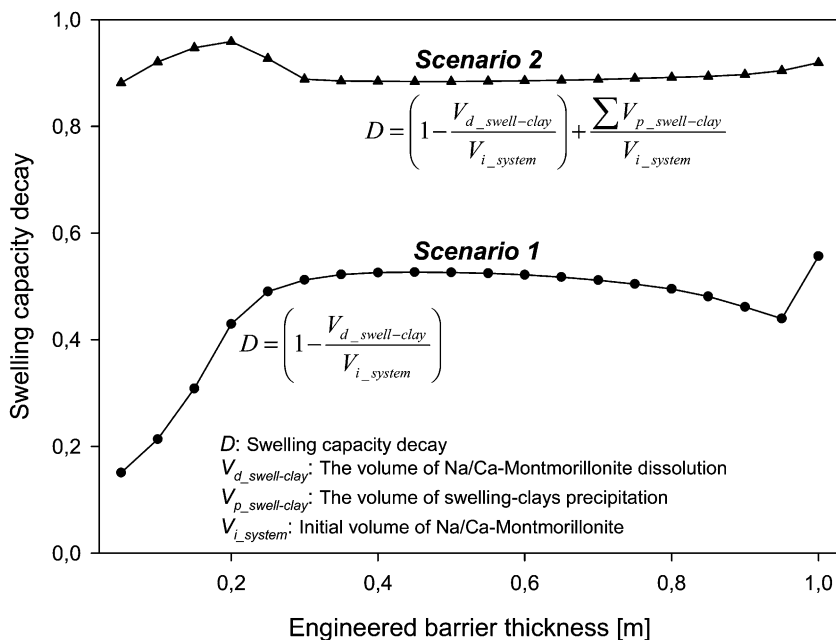
Fig. 6. Swelling capacity decay of the engineered barrier after 3320 years of reaction and transport. Scenario (1) Na/Ca-montmorillonite chemical transformation with prediction of the non-swelling clays neo-formation. Scenario (2) Na/Ca-montmorillonite chemical transformation with prediction of the swelling clays neo-formation (process identified in this study).

proportional on the Na/Ca-montmorillonite transformation. Therefore, the Eq. (2) can be explained as

$$D = \left(1 - \frac{V_{d\_montmorillonite}}{V_{i\_montmorillonite}}\right). \tag{5}$$

This means that the decay of swelling capacity is equal to zero ($D = 0$) when the montmorillonite is completely transformed ($V_{d\_montmorillonite} = V_{i\_montmorillonite}$).

(2) In contrast, the second scenario considers the progressive chemical transformation of Na/Ca-montmorillonite with prediction of the *swelling minerals neo-formation* (process identified in our simulations). It follows therefrom that the decay of swelling capacity of the bentonite barrier is partially or totally compensated with the neo-formed swelling clays. The decay of swelling capacity can be then calculated by using the Eq. (2)

Fig. 6 shows the swelling capacity decay of the engineered barrier for these two scenarios. In fact, the swelling capacity of the bentonite barrier was not drastically affected after 3320 years of reaction and transport because the volume of neo-formed swelling-clays is almost directly proportional on the volume of transformed Na/Ca-montmorillonite.

A graphical method was used in order to estimate the swelling capacity decay until a complete chemical trans-

formation of Na/Ca-montmorillonite in the system. This method is summarized by three stages:

(1) It was assumed a *quasi-stationary state*. The Fig. 7 shows that effectively the pH variation between 3070 and 3320 years is small in each reactive-cell of the engineered barrier. However, this system state could be transitory because in the boundaries of the barrier there is a constant perturbation.

(2) The second stage takes into account a *linear graphic extrapolation* to estimate the minimal and maximal time to which the Na/Ca-montmorillonite is completely transformed in the system (see Fig. 8).

(3) The final stage takes also into account a *linear graphic extrapolation* by using as limits the minimal and maximal time estimated in the previous stage. Now, to estimate the swelling capacity decay until a complete transformation of Na/Ca-montmorillonite in the system (see Fig. 9). In this case, the swelling capacity decay of the engineered barrier is calculated by the following equation:

$$D = \frac{\sum V_{p\_swell\text{-}clay}}{V_{i\_montmorillonite}}, \tag{6}$$

where $V_{p\_swell\text{-}clay}$ is the volume of the swelling-clay neo-formed and the $V_{i\_montmorillonite}$ the initial volume of Na/Ca-montmorillonite in the system.
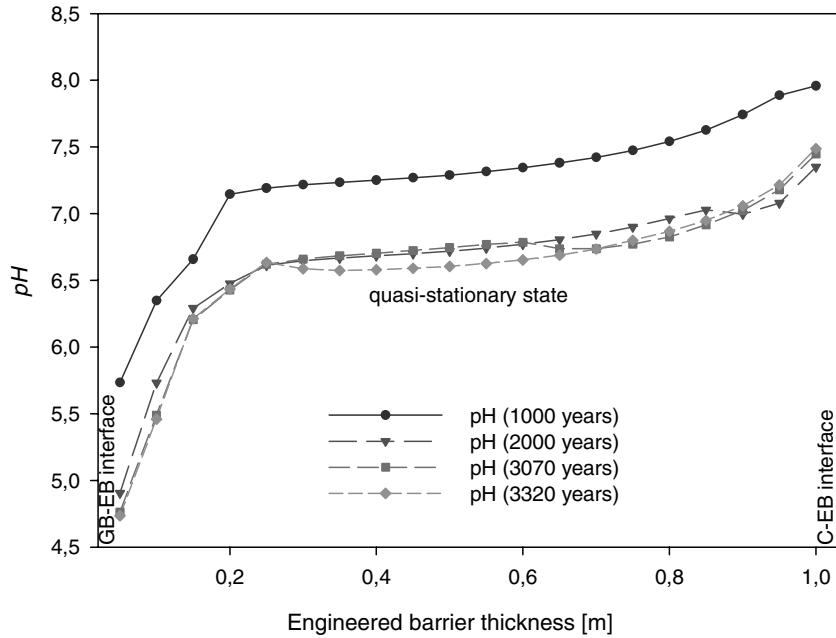
Fig. 7. pH evolution of the fluid interaction in the engineered barrier after 1000, 2000, 3070 and 3320 years of reaction and transport.

This very simplified method allows to predict that the decay of swelling capacity of engineered barrier lies between 11% and 14% when the Na/Ca-montmorillonite is completely transformed in the system (see Fig. 9).

This simple extrapolation approach was used to show how in the worst of cases for this modeling study, the bentonite barrier conserve the swelling properties. Evidently, this approach do not allow to extrapolate the

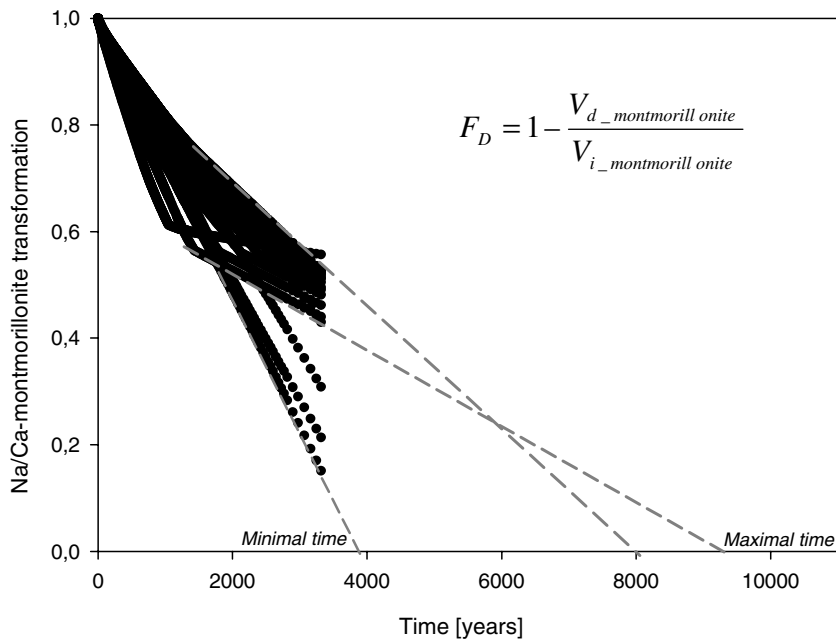$$F_D = 1 - \frac{V_{d\_montmorill\ onite}}{V_{i\_montmorill\ onite}}$$

Fig. 8. Linear extrapolation to calculate the minimal and maximal time to which the Na/Ca-montmorillonite is completely transformed (graphical method).
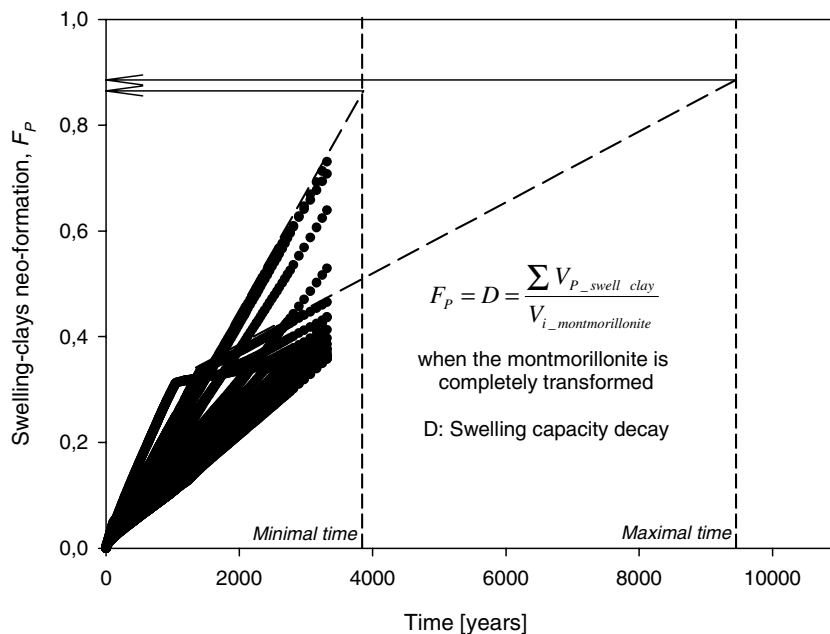
Fig. 9. Linear extrapolation to calculate the swelling capacity decay after a complete Na/Ca-montmorillonite transformation (graphical method).

chemical transformations of bentonite barrier in the long-term (ex. 100,000 and 1,000,000 years).

The precedent Fig. 7 shows also that the pH is not homogeneous in the engineered barrier. In general, an acid pH was observed near of the geological medium boundaries. This pH fall is due to a significant [H$^+$] accumulation in the system produced by the hydrolysis reactions of chlorites and saponites. It is important to remark that a constant concentration of total iron in the boundaries of container also produces an acidification phenomenon. This limitation suggests to take into account the corrosion process by using a dissolution reaction in reducing conditions:

$$Fe^0 + 2H_2O \Longleftrightarrow Fe^{++} + 2OH^- + H_2 \uparrow$$
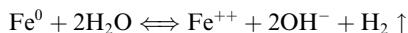
6. Conclusion

The chemical transformations occurring in a bentonite barrier for radioactive waste confinement depend directly on the reaction temperature, the rate of iron corrosion, the composition of interaction fluid, the nature and/or amount of accessory minerals, the diffusion coefficients of solutes, the reactive surface area of minerals, the texture of porous media, etc. At the present time, it is still difficult to consider efficiently all parameters in a same modelling, because of the complexity for their estimation. For this reason, the KIRMAT simulations were carried out under drastic conditions of radioactive waste repository:

(1) There is an infinite source and constant concentration of major cations in the boundaries of the geological medium. A constant concentration of total iron was also considered in the boundaries of container but limited arbitrary at 1000 years.
(2) Temperature of reaction, reactive surface area of minerals, diffusion coefficients of solutes and porosity were considered constants as a function of time-space.

The results show that Na/Ca-montmorillonite-to-Ca-montmorillonite conversion is the main chemical transformation in the bentonite barrier. A minimal neo-formation of illite, saponites, chlorites, and sodium-montmorillonite was also observed in this barrier.

A simplified method shows that the swelling capacity of the engineered barrier is not drastically affected after 3320 years of reaction and transport because the volume of neo-formed swelling-clays is almost directly proportional on the volume of transformed Na/Ca-montmorillonite. In fact, a graphical method predicts that under our hypothesis the decay of swelling capacity of engineered barrier lies between 11% and 14% when the Na/Ca-montmorillonite is completely transformed in the system (cation exchange + minimal geochemical transformation).

Acknowledgement

References

Bajracharya, K., Barry, D.A., 1993. Mixing cell models for nonlinear equilibrium single species adsorption and transport. Journal of Contaminant Hydrology 12, 227–243.

Bertrand, C., Fritz, B., Sureau, J-F., 1994. Hydrothermal experiments and themo-kinetic modelling of water–sandstone interactions. Chemical Geology 116, 189–202.

Chermak, J.A., Rimstidt, 1989. Estimating the thermodynamic properties (ΔG_f^0 and ΔH_f^0) of silicate minerals at 298 K from the sum of polyhedral contributions. American Mineralogist 74, 1023–1031.

Chermak, J.A., Rimstidt, 1990. Estimating the free energy of formation of silicate minerals at high temperatures from the sum of polyhedral contributions. American Mineralogist 75, 1376–1380.

Collin, F., Li, X.L., Radu, J.P., Chalier, R., 2002. Thermo-Hydro-mechanical coupling in clay barriers. Engineering Geology 64, 179–193.

Fritz, B., 1975. Etude themodynamique et simulation des réactions entre minéraux et solutions. Application à la géochimie des altérations et des eaux continetales. Mém. Sci. Géol., v. 41, Strasbourg, France, 153 p.

Fritz, B., 1981. Etude thermodynamique et modélisation des réactions hydrothermales et diagénétiques. Mém. Sci. Géol. 65, 197.

Fritz, B., Tardy, Y., 1976. Séquence de minéraux secondaires dans l'altération des granites et roches basiques: modèles thermodynamiques. Bulletin of the Soceity of Géology France 18, 7–12.

Gens, A., Guimaraes, L., do, N., Garcia-Molina, A., Alonso, E.E., 2002. Factors controlling rock–clay buffer interaction in a radioactive waste repository. Engineering Geology 64, 297–308.

Gérard, F., Clement, A., Fritz, B., 1998. Numerical validation of a Eulerian hydrochemical code using a 1D multisolute mass transport system involving heterogeneous kinetically controlled reactions. Journal of Contaminant Hydrology 30, 201–216.

Guillaume, D., 2002. Etude expérimentale du système fer-smectite en présence de solution à 80 °C et 300 °C. PhD Thesis, Henri Poincaré University, Nancy I, France, 210 p.

Helgeson, H.C., Brown, T.H., Nigrini, A., Jones, T.A., 1970. Calculations of mass transfer in geochemical processes involving aqueous solutions. Geochimica et Cosmochimica Acta 34, 569–592.

Hökmark, H., 2004. Hydration of the bentonite buffer in a KBS-3 repository. Applied Clay Science 26, 219–233.

Hökmark, H., Karnland, O., Pusch, R., 1997. A technique for modeling transport/conversion processes applied to smectite-to-illite conversion in HLW buffers. Engineering Geology 47, 367–378.

Jacquot, E., 2000. Modélisation thermodynamique et cinétique des réactions géochimiques entre fluides de bassin et socle cristallin. PhD Thesis, Louis Pasteur University, Strasbourg I, France, 202 p.

Jacquot, E., 2002. Composition des eaux interstitielles des argilites du Callovo-Oxfordien non perturbées. Rapport ANDRA No. D NT ASTR 02-041, 13 p.

Källvenius, G., Ekberg, C., 2003. TACK – a program coupling chemical kinetics with a two-dimensional transport model in geochemical systems. Computers Geosciences 29, 511–521.

Keijzer, Th.J.S., Kleingeld, P.J., Loch, J.P.G., 1999. Chemical osmosis in compacted clayed material and the prediction of water transport. Engineering Geology 53, 151–159.

Kluska, J.M., 2001. Modélisation Thermodynamique et Cinétique des Réactions Géochimiques dans une Barrière Ouvragée en Bentonite. Simulations dans des conditions réductrices, de 60 à 180 °C en l'absence et en présence d'une source de fer sur une durée de 20 ans. Rapport ANDRA No. CRP 0CGS 01-004, 34 p.

Kluska, J.M., Fritz, B., Clement, A., 2002. Predictions of the mineralogical transformations in a bentonite barrier surrounding an iron radioactive container. International meeting "Clay in natural and engineered barriers for radioactive waste confinement" ANDRA, 8–12 December 2002, Reims, France.

Komine, H., 2004. Simplified evaluation for swelling characteristics of bentonites. Engineering Geology 71, 265–279.

Komine, H., Ogata, N., 2003. New equations for swelling characteristics of bentonite-based buffer materials. Canadian Geotechnical Journal 40, 460–475.

Le Gallo, Y., Bildstein, O., Brosse, E., 1998. Coupled reaction-flow modelling of diagenic changes in reservoir permeability, porosity and mineral compositions. Journal of Hydrology 209, 366–388.

Lehikoinen, J., Carlsson, J., Muurinen, A., Olin, M., Salonen, P., 1996. Evaluation of factors affecting diffusion in compacted bentonite. Materials Research Society Symposium Proceedings 412, 675–682.

Madé, B., Clément, A., Fritz, B., 1994. Modelling mineral/solution interactions: The thermodynamic and kinetic code KINDISP. Computers & Geosciences 20 (9), 1347–1363.

Malusis, M.A., Shackelford, C.D., 2002. Theory for reactive solute transport through clay membrane barriers. Journal of Contaminant Hydrology 59, 291–316.

Montes-H, G., 2002. Etude expérimentale de la sorption d'eau et du gonflement des argiles par microscopie électronique à balayage environnementale (ESEM) et analyse digitale d'images. PhD Thesis, Louis Pasteur University, Strasbourg I, France.

Montes-H, G., Geraud, Y., 2004. Sorption kinetic of water vapour of MX80 bentonite submitted to different physical-chemical and mechanical conditions. Colloids and Surfaces A: Physicochemical Engineering Aspects 235, 17–23.

Montes-H, G., Duplay, J., Martinez, L., Mendoza, C., 2003. Swelling-shrinkage kinetics of MX80 bentonite. Applied Clay Science 22, 279–293.

Montes-H, G., Fritz, B., Clement, A., 2004. Modeling of transport and reaction in an engineered barrier for radio-

active waste confinement. Rapport ANDRA, CRP 0 CGS 04001, 61 p.

Nagy, K.L., Cygan, R.T., Hanchar, J.M., Sturchio, N.C., 1999. Gibbsite growth kinetics on gibbsite, kaolinite, and muscovite: atomic force microscopy evidence for epitaxy and assessment of reactive surface area. Geochimica et Cosmochimica Acta 63 (16), 2337–2351.

Neaman, A., Pelletier, M., Villieras, F., 2003. The effects of exchanged cations, compression, heating and hydration on textural properties of bulk bentonite and its corresponding purified montmorillonite. Applied Clay Science 22, 153–168.

Noack, Y., Collin, F., Nahon, D., Delvigne, J., Michaux, L., 1993. Secondary-mineral formation during natural weathering of pyroxene: review and thermodynamic approach. American Journal of Science 293, 111–134.

Poinssot, C., Toulhoat, P., Goffé, B., 1998. Chemical interaction between a simulated nuclear waste glass and different backfill materials under a thermal gradient. Applied Geochemistry 13 (6), 715–734.

Sauzeat, E., Guillaume, D., Neaman, A., Dubessy, J., François, M., Pfeiffert, C., Pelletier, M., Ruch, R., Barres, O., Yvon, J., Villéras, F., Cathelineau, M., 2001. Caractérisation minéralogique, cristallochimique et texturale de l'argile MX80. Rapport ANDRA No. CRP0ENG 01-001, 82 p.

Savage, D., Noy, D., Mihara, M., 2002. Modelling the interaction of bentonite with hyperalkaline fluids. Applied Geochemistry 17, 207–223.

Tournassat, C., Neaman, A., Villiéras, F., Bosbach, D., Charlet, L., 2003. Nanomorphology of montmorillonite particles: estimation of the clay edge sorption site density by low pressure gas adsorption and AFM observations. American Mineralogist 88, 1989–1995.

Ulm, F.J., Heukamp, F.H., Germaine, J.T., 2002. Residual design strength of cement-based materials for nuclear waste storage systems. Nuclear Engineering and Design 211, 51–60.

White, A.F., Peterson, M.L., 1990. Role of reactive-surface-area characterization in geochemical kinetic models. In: Melchior, D., Bassett, R. (Eds.), Chemicals modelling of aqueous systems II: Assoc. Chem. Soc. Symp. Series, 41, pp. 461–475.